Synergistic Flame Retardant Effect of Poly(ether sulfones) and Polysiloxane on Polycarbonate

Shu-Mei Liu,[1] Yan Yang,[1] Zhi-Jie Jiang,[2] Yan-Hui Zhou,[1] Jian Zuo,[2] Jian-Qing Zhao[1]

[1]*College of Materials Science and Engineering, South China University of Technology, 510640 Guangzhou, China*
[2]*The Key Lab of GD for High Property and Functional Macromolecular Materials, South China University of Technology, 510640 Guangzhou, China*

ABSTRACT: Flame retardance of bisphenol A polycarbonate (PC) was improved by the co-addition of poly (ether sulfones) (PES) and polysiloxane/acrylate copolymer (PSiA) while retaining a high rigidity and toughness. A UL 94 V-0 rating for 1.6-mm thick samples of PC/PES/PSiA blend with 10.0 wt % PES and 0.5 wt % PSiA (PC/10PES/0.5PSiA) was obtained. Its average heat release rate (av-HRR) in a cone calorimeter measurement was decreased by 19% on the basis of PC/PES blend with 10.0 wt % PES. Scanning electron microscopy (SEM) morphologies of impact-fractured surfaces revealed that the incorporation of 0.5 wt % PSiA decreased the dimensions of PES dispersed phase and provoked the uniform distribution of PES in PC matrix. Thermogravimetric-Fourier transform infrared spectroscopy analysis results revealed that PSiA dominantly promoted the degradation of PC and the degraded products were combined with PES to form a superior flame-retarded carbon layer. A higher sulfur and silicon content on the residue surface after vertical burning tests detected by SEM/energy dispersive spectrometer signified their accumulation during combustion. © 2011 Wiley Periodicals, Inc. J Appl Polym Sci 124: 4502–4511, 2012

Key words: polycarbonate; poly(ether sulfones); polysiloxanes; flame retardance; modification

INTRODUCTION

Recently, halogen-free flame retardant technologies of bisphenol A polycarbonate (PC) have been extensively developed together with environmental considerations.[1] It has been a common practice to incorporate sulfonate salts such as potassium diphenylsulfone sulfonate (KSS), potassium perfluorobutane sulfonate, and sodium 2,4,5-trichlor benzene sulfonate into PC to modify the flame retardance.[2,3] Commercially available KSS induces 3.2-mm thick specimens of PC to pass UL 94 V-0 rating even at as low as 0.1 wt % loading.[4] However even small amounts of KSS bring about poor resistance of PC to hydrolysis and its use is not satisfactory especially in thin wall articles with a thickness of less than 2.5 mm. Additional substitutes for sulfonate salts need to be further sought. It is regarded that desulfonated products of sulfonate salts, i.e., SO_2, water, and sulfurous acid accelerate thermal degradation of PC to ensure the formation of an insulating flame retardant carbon layer on the surface.[5,6] It seems all sulfur-containing substance is potentially available for promoting the charring of PC. As a high-performance thermoplastic polymer, poly(ether sulfones) (PES) contains sulfone unit with 10 wt % of sulfur content and self-extinguishes in air with 38% of the limiting oxygen index (LOI). Thermal degradation of PES generates large amounts of SO_2 as a one-stage main-chain random scission.[7,8] Moreover PES can endow PC with excellent mechanical properties and resistance to high temperature, chemical corrosion, and ignition when blended with PC. Mechanical properties and phase inversion behavior of PC/PES blends have been investigated.[9,10] To our knowledge, however, no study has reported a flame retardant function of PES in PC. It is an attractive approach that PES is employed as an alternative for KSS to enhance the flame retardance of PC.

Recently, silicones[11] such as polyhedral oligomeric silsesquioxane (POSS)[12] and polydimethylsiloxane[13] have shown great potentials of simultaneously improving the thermal and flame retardant properties of polymeric materials. Polysiloxanes were particularly effective in flame-retarding PC by migrating to the surface to form a highly flame-resistant char during combustion.[14] Together with sulfonate salts,

polysiloxanes significantly elevate the UL 94 rating and reduce the generation of smoke, heat, and toxic carbon monoxide gas during PC combustion.[15] A polysiloxane/acrylate copolymer is regarded as being compatible with PC[16] and its combination with PES is desirable to produce a noticeable flame retardant effect on PC. The synergistic flame retardant behavior and mechanism of two additives on PC are investigated in the present article.

EXPERIMENT

Materials

PC (L1250Y, Teijin, Singapore) and polytetrafluoroethylene (PTFE, Teflon 6C, Du Pont, Wilmington) were used. PES was supplied by BASF (Ultrason E2010 Berlin, Germany). The synthesis of polysiloxane/acrylate copolymer (PSiA) according to the Ref. 17: first polysiloxane latex was prepared by the addition of 8 : 2 : 0.5 (molar ratio) of phenyltriethoxysilane, octamethylcyclotetrasiloxane, and γ-methacryloxypropyltrimethoxysilane in the presence of dodecyl benzene sulfonic acid and octylphenol polyoxyethylene ether at 50°C for 8 h. Then the latex was grafted by equimolar amounts of butyl acrylate and methyl methacrylate at 75°C for 4 h. The weight ratio of polysiloxane and polyacrylate was about 6 : 4. The chemical structures of PES and PSiA are illustrated in Scheme 1.

Specimen preparation

Initially, PC and PES were dried in an oven at about 105 and 150°C, respectively, for 5 h. The mixture of PC, PES, PSiA, and PTFE was melt-kneaded and extruded into pellets in a 30-mm twin-screw extruder with a cylinder temperature of 285–300°C at a screw speed of 100 rpm. The resultant pellets were dried at 105°C for 5 h and then injection-molded at 290–310°C into test pieces.

Characterization

LOI (Fire Testing Technology Ltd., UK) measurements were performed according to ASTM D 2863-2000 method. Vertical burning tests were carried out using a UL 94 flammability meter (Fire Testing Technology Co. Ltd., UK) according to UL 94 classification. The fire performance under forced flaming conditions was characterized by the cone calorimeter (Fire Test Technology Co. Ltd., UK) according to ISO5660-1 (2000) under an external heat flux of 35 W/m^2 with $100 \times 100 \times 6$ mm^3 samples. Tensile strength of specimens was determined according to ASTM D638-2003 and flexural strength according to ASTM D790-2003 using a Shimadzu (AG-1) universal electronic tensile testing machine. Izod notched impact strength of specimens was determined using a Zwick 5102 pendulum type testing machine according to ASTM D256-2006.

Thermogravimetric analysis (TGA) was performed on a NETZSCH TG209F1 thermal analyzer at a heating rate of 20°C/min under nitrogen atmosphere. Thermogravimetric-Fourier transform infrared spectroscopy (TGA-FTIR) was carried out using a NETZSCH STA449C TG instrument connected to a BRUKER TENSOR27 FTIR. Observation of the char surface morphologies was carried out using a NOVA NANOSEM 430 scanning electron microscopy (SEM) and energy dispersive spectrometer (EDS) analysis was accomplished using an ADD350+HKL Fast EBSD system attached to the SEM.

RESULTS AND DISCUSSION

Effect of PES on the properties of PC

PC quickly self-extinguishes in air due to a relatively strong tendency to charring, exhibiting a V-2 rating with 3.2-mm thick specimens in UL 94 test. PES is highly flame retardant materials with 38% of LOI value and exhibits V-0 rating with 1.6-mm thick specimens. Both PC and PES are amorphous engineering polymers. Melting temperature of PC is 220–
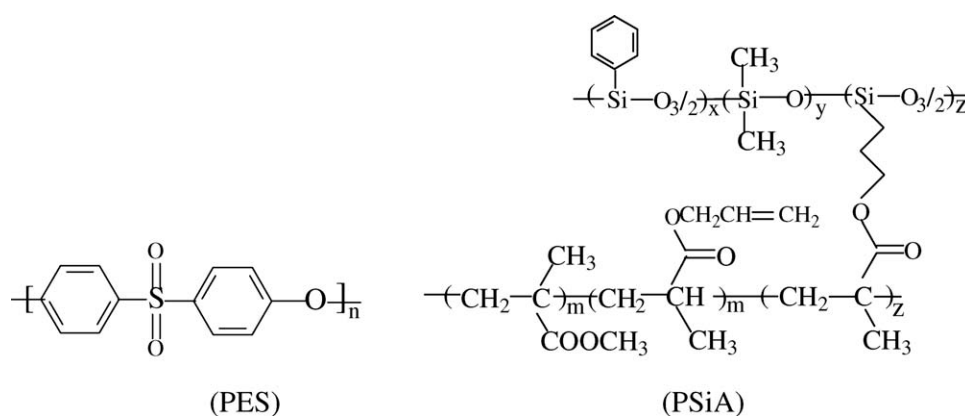
Scheme 1 The chemical structures of PES and PSiA.

TABLE I
Mechanical and Flame-Retarded Properties of PC/PES Blends
with Different PES Loadings

Properties	A1	A2	A3	A4	A5	A6
PC (wt %)	99.7	97.7	94.7	89.7	84.7	79.7
PES (wt %)	0	2.0	5.0	10.0	15.0	20.0
PTFE (wt %)	0.3	0.3	0.3	0.3	0.3	0.3
Tensile strength (MPa)	59.4	60.1	60.4	60.4	61.7	63.8
Elongation at break (%)	111	105	103	101	100	96
Izod impact strength (J m^{-1})	901	887	894	871	154	133
Flexural strength (MPa)	91.0	91.2	91.2	91.8	94.1	94.6
UL 94 rating at 3.2-mm thickness	V-2	V-1	V-0	V-0	V-0	V-0
LOI (%)	26.0	30.5	32.9	33.7	34.5	34.8

230°C and that of PES is as high as 320–330°C with large melt viscosity. The processing temperature of PC/PES blends was controlled below 310°C to prevent from the degradation of PC. Since more than 20 wt % of PES loading led to extruding difficulties, PES in 2.0, 5.0, 10.0, 15.0, and 20.0 wt % loadings was blended with PC in the presence of 0.3 wt % of PTFE which behaved as preventing flammable drips during combustion.

Flame-retarded and mechanical properties of the obtained blends have been measured and the results are contained in Table I. It is found that PES causes a sensible increment in LOI values of PC, and the PC/PES blend with 5.0 wt % PES composition passes V-0 rating with 3.2-mm thick specimens. But it is still difficult for 1.6-mm specimens of PC/PES blends to pass V-0 rating even though PES loadings go up to 20 wt %. Less than 10 wt % PES has the least detrimental effect on mechanical properties of PC while a further increase in PES loadings causes severe decrease in Izod impact strength of PC. The Izod impact strength of the blend with 15.0 wt % PES (A5) decreases from 871 J/m with 10.0 wt % PES (A4) to 154 J/m whereas the tensile strength and flexural strength raise from 60.4 and 91.8 MPa to 61.7 and 94.1 MPa, respectively. As a result, a modified flame retardance for PC is obtained by the addition of 5–10 wt % PES while retaining a high toughness.

Effect of PES and PSiA on the properties of PC

Single PSiA in 0.1, 0.2, 0.5, 1.0, and 2.0 wt % loadings was incorporated into PC. It is found that the

LOI values of PC hardly increase and UL 94 rating is not elevated even though the loading of PSiA achieves 2.0 wt %. In addition, more than 2 wt % of PSiA can abate the toughness of PC. PES and PSiA were simultaneously employed to flame-retarding for PC. Together with 0.2 wt % PSiA, PES in 1.0, 3.0, 5.0, 8.0, and 10.0 wt % loadings was added to PC, respectively. A comparison of flame-retarded properties of the formed PC/PES/PSiA blends (FR1, FR2, FR3, FR4, FR5) is shown in Table II. A slow increase in LOI values of various blends is found with PES loadings. FR1, FR2, and FR3 with less than 5 wt % PES obtain V-1 while FR4 and FR5 with more than 8 w t% PES pass V-0 for 1.6-mm thick specimens, indicating that PES is synergistic with PSiA to impart flame retardance to PC. At the meantime, the high toughness and rigidity of PC are retained for five blends. Otherwise, the co-addition of 0.5 wt % PSiA and 10.0 wt % PES (FR6, PC/10PES/0.5PSiA) cannot further upgrade the UL 94 rating and FR7 with 1.0 wt % PSiA only passes a V-1 rating for 1.6-mm thick specimens. More than 1.0 wt % of PSiA loadings would adversely influence the flame retardance of PC/10PES. Thus it is available to advance the flame-retarded rating of PC by the combination of small amounts of PSiA with PES on the basis of maintaining excellent mechanical properties of PC.

Measurements were performed to evaluate the flammability characteristics of various blends under forced flaming conditions by a cone calorimeter. The data of peak heat release rate (pk-HRR), average heat release rate (av-HRR), average effective heat combustion (av-EHC), average mass loss rate (av-MLR), and

TABLE II
Flame-Retarded Properties of PC/PES/PSiA Blends

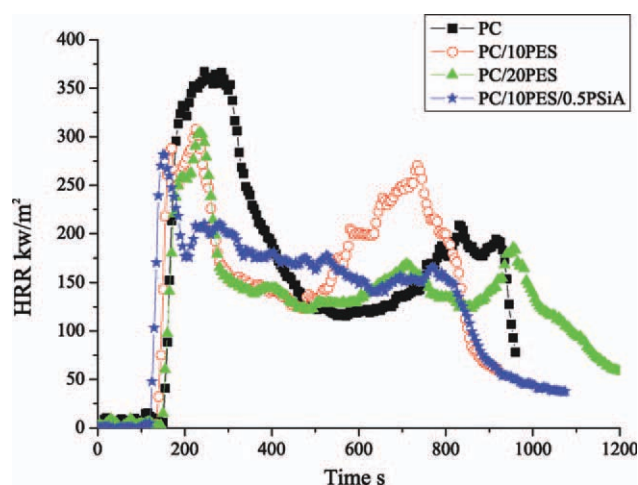|	FR1	FR2	FR3	FR4	FR5	FR6	FR7
PC (wt %)	98.5	96.5	94.5	91.5	89.5	89.2	88.7
PES (wt %)	1.0	3.0	5.0	8.0	10.0	10.0	10.0
PSiA (wt %)	0.2	0.2	0.2	0.2	0.2	0.5	1.0
PTFE (wt %)	0.3	0.3	0.3	0.3	0.3	0.3	0.3
UL 94 rating at 1.6-mm thickness	V-1	V-1	V-1	V-0	V-0	V-0	V-1
LOI (%)	31.3	32.5	33.8	34.0	34.2	34.3	34.0

TABLE III
Cone Calorimetry Data for Two PC/PES Blends and PC/10PES/0.5PSiA

	pk-HRR (kW/m^2)	av-HRR (kW/m^2)	av-EHC (MJ/kg)	av-MLR [g/s($\times$100)]	THR (MJ/m^2)
PC	367.2	191.1	26.0	6.5	159.7
PC/10PES (A4)	307.6	180.2	23.1	6.8	141.2
PC/20PES (A6)	304.4	139.1	24.7	5.0	155.0
PC/10PES/0.5PSiA (FR6)	281.6	145.4	23.7	5.4	139.5

total heat release (THR) of the PC, PC/10PES (A4), PC/20PES (A6), and PC/10PES/0.5PSiA (FR6) samples are summarized in Table III. HRR traces as a function of time are shown in Figure 1. Pk-HRR and av-HRR values of neat PC are 367.2 and 191.1 kW/m^2, and an addition of 10.0 wt % PES evokes the two values of PC to go down to 307.6 and 180.2 kW/m^2. Moreover av-HRR of PC/PES blends discloses a remarkable decline with PES loadings. Pk-HRR value of PC/10PES/0.5PSiA is 281.6 kW/m^2 which is lower than 304.4 kW/m^2 of PC/20PES and av-HRR value is 145.4 kW/m^2, close to 139.1 kW/m^2 of PC/20PES. A 19% reduction in av-HRR value based on PC/10PES indicates that small amounts of PSiA apparently generate synergistic flame retardance with PES. The MLR parameter in combustion is primarily responsible for HRR of a material. Av-MLR of PC/10PES/0.5PSiA reduces from 0.068 g/s of PC/10PES to 0.054 g/s and the variation in av-MLR between two blends presents a similar trend as in av-HRR. Nevertheless, no evident decrease in av-EHC and THR parameter of PC/10PES is induced by 0.5 wt % PSiA. The above results confirm that the co-addition of PES and PSiA obviously declines the flammability characteristics of PC.

Morphology analysis of impact-fractured surfaces

Uniform dispersion of several synergistic compositions in the matrix is the substantial premise of an excellent flame retardant effect. It is difficult to identify the presence of PSiA owing to low loadings, hence the distribution of PES is principally considered. SEM micrographs of impact-fractured surface of PC/10PES and PC/20PES are shown in Figure 2. It is found that both PC/10PES and PC/20PES show pronounced droplet/matrix morphologies with spherical PES particles in PC matrix. Moreover, reserved cavities can be discerned after spherical PES particles are drawn out during sudden impacts. The presence of interfaces manifests little adhesion and immiscibility between PC and PES phases, which result in a poor dispersion and a broad size distribution of PES particles. For PC/20PES, the diameter of PES particles changes in the range 0.5–5 μm. Elemental distribution of the matrix and the dispersed phase for PC/20PES obtained from SEM/EDS (Fig. 3) is listed in Table IV. The evident contrast of sulfur content (0 vs. 4.52%) further illuminates the irregular distribution of PES. Phase structure coarsening accounts for a noticeable decrease in considered properties,[18] and is the main reason why the addition of 20.0 wt % PES cannot further upgrade the flame retardance of PC.

SEM morphologies of impact-fractured surface of PC/10PES/0.5PSiA are displayed in Figure 4. PES particles seem to be anchored much firmly in the PC continuous phase and the adhesion between PC and PES components is modified by the incorporation of 0.5 wt % PSiA. In addition, most of PES particles are less than 1 μm and their dimension distribution becomes narrow. Uniform dispersion of PES particles in PC matrix should aid the improvement of the flame retardance. Compared with PC/10PES, as a result, the UL 94 rating of PC/10PES/0.5PSiA is upgraded to V-0 rating with 1.6-mm thick specimens and av-HRR in a cone calorimeter measurement is decreased by 19%.

Figure 1 Cone calorimetry traces of PC, two PC/PES blends and PC/10PES/0.5PSiA. [Color figure can be viewed in the online issue, which is available at wileyonlinelibrary.com.]

Thermogravimetric analysis

Thermal degradation of PC, PES, and two PC/PES blends was assessed by thermogravimetric analysis in nitrogen atmosphere and their TGA and derivative thermogravimetric analysis (DTG) curves are compared in Figure 5. It can be seen that both PC and PES behave as a one-stage degradation pathway
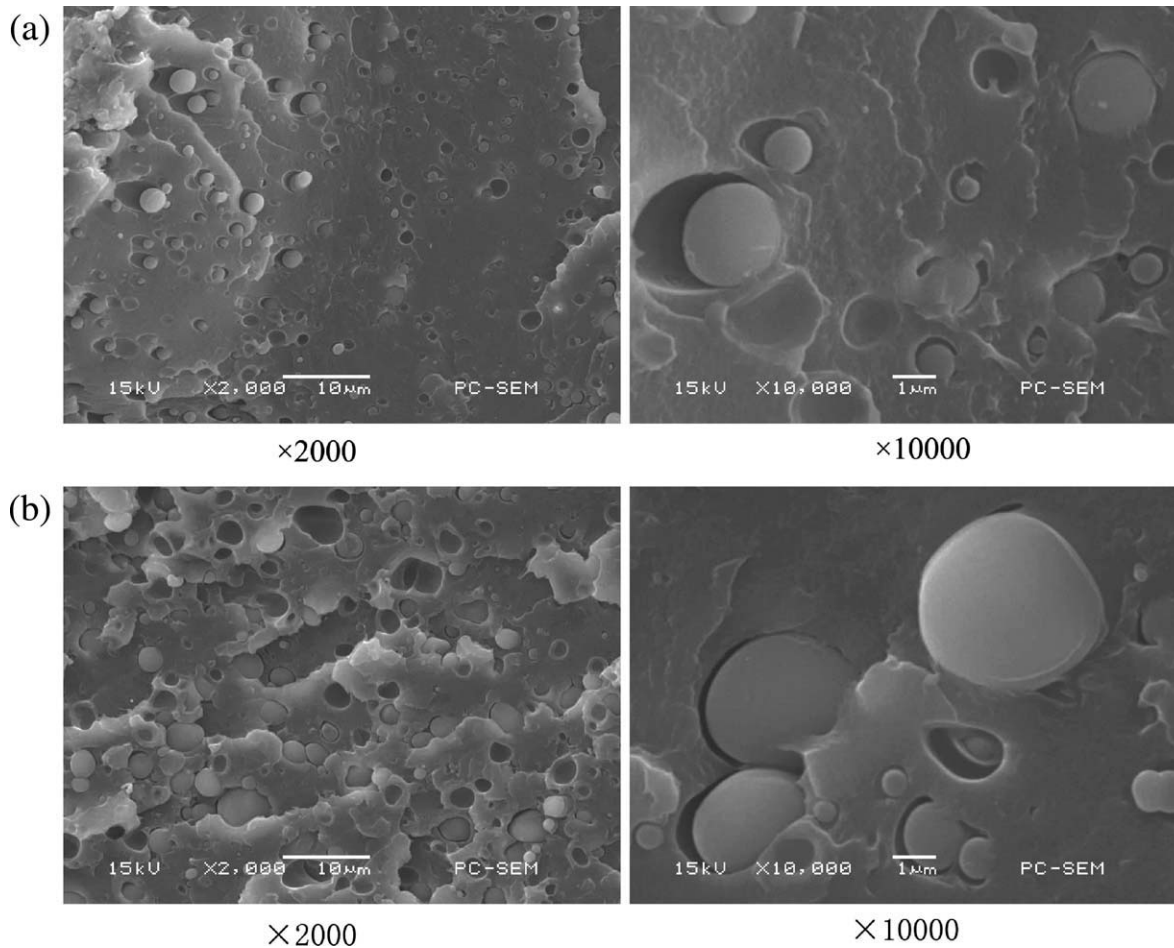
Figure 2 SEM micrographs of impact-fractured surfaces of PC/10PES (a) and PC/20PES (b) at different magnifications.
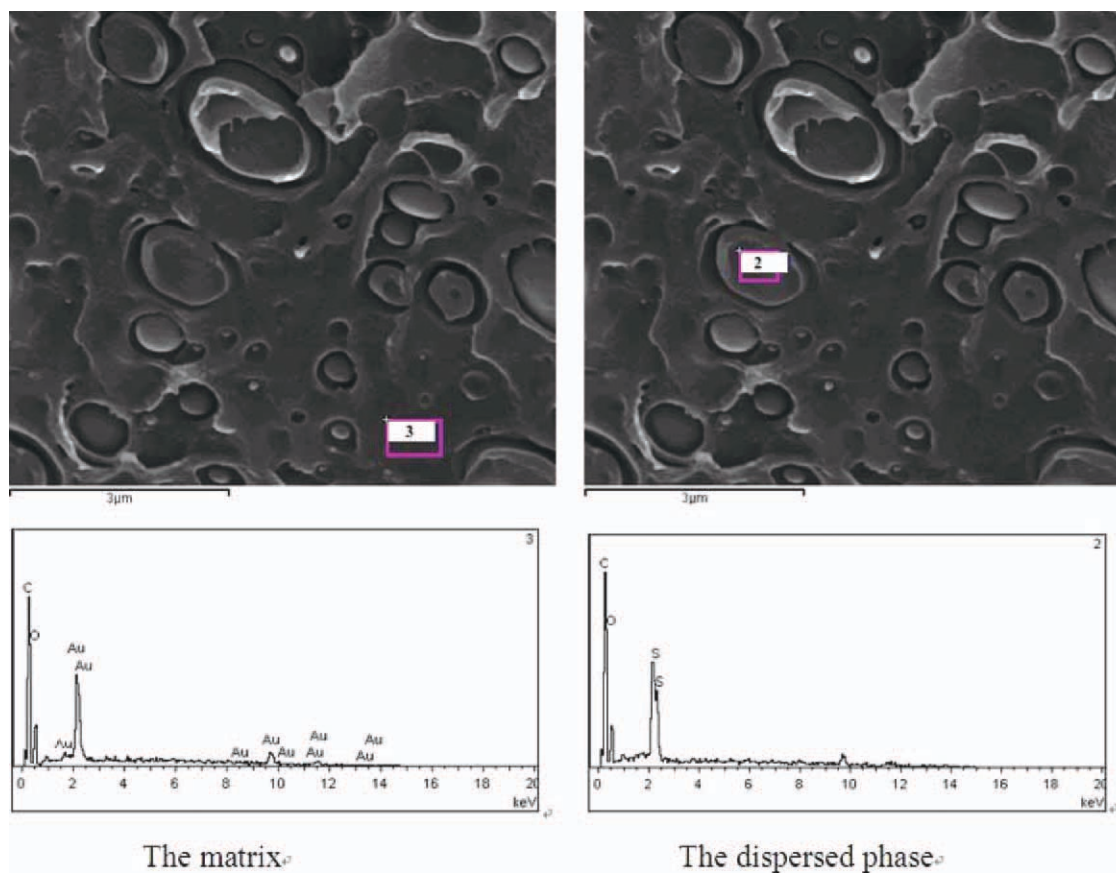

Figure 3 SEM/EDS micrographs of impact-fractured surface of PC/20PES. [Color figure can be viewed in the online issue, which is available at wileyonlinelibrary.com.]

TABLE IV
Elements Analysis of the Matrix and the Dispersed Phase of PC/20PES

Elements	Weight (%)		
	C	O	S
Matrix	52.28	18.88	0
Dispersed phase	69.29	26.19	4.52

and the main degradation of PC and PES occurs at 500–550°C and 525–600°C, respectively. Five percent weight loss weight temperature ($T_{5\%}$) is used for representing an initial degradation temperature. $T_{5\%}$ of PES is 526.0°C which is 45.8°C higher than that of PC. The char yield of PES at 650°C achieves 42.4%, which is higher than 22.7% of PC. PES possesses higher thermal stability and charring capability.

Both PC/10PES and PC/20PES blends exhibit a one-stage degradation pathway and the initial degradation temperature of PC is elevated by PES. The addition of 10.0 wt % PES leads to 11.7 and 9.0°C increase in $T_{5\%}$ and the temperature of the maximum weight loss rate (T_{max}) of PC. $T_{5\%}$ and T_{max} go up slightly with PES loadings up to 20.0 wt %. Furthermore, the maximum weight loss rate of PC/10PES and PC/20PES is larger than that of PC or PES, maybe attributed to SO_2 from the decomposition of PES which accelerates the PC degradation.[5,6] It was thought that flame retardance of PC at small-case fire tests such as LOI and UL 94 increased with the weight loss quickened.[3] The char yield of the blends at 650°C increases slightly with PES loadings. Therefore it is proposed that a higher thermal stability and a larger weight loss rate are responsible for the improvement of flame retardance of PC.

TGA and DTG curves of PSiA in nitrogen atmosphere are depicted in Figure 6. PSiA shows a two-stage degradation and $T_{5\%}$ appears at 332°C. The first main degradation takes place over the temperature range 350–450°C and T_{max} at 390°C. Degradation products are mainly H_2O and acrylate-like compounds which are capable of accelerating the PC degradation. The second main degradation originating from the scission of methyl and phenyl groups attached to Si—O—Si chain[19] occurs from 460 to 530°C, which locates in the degradation temperature regions of PC. Nearly 79% of total mass loss occurs up to 650°C.

TGA and DTG curves of two PC/10PES/PSiA in nitrogen atmosphere are contrasted with those of PC and PC/10PES in Figure 7. T_{max} of PC/10PES/0.2PSiA and PC/10PES/0.5PSiA is 7.7 and 40.3°C lower than that of PC. More than 0.5 wt % of PSiA renders more severe degradation of PC and PES. Because the degradation at too low temperature would result in easy spreading of the flame on the surface to correspondingly abate the flame retardance, PC/10PES/0.2PSiA and PC/10PES/0.5PSiA exhibit V-0 while PC/10PES/1.0PSiA exhibits V-1 at 1.6-mm thickness as listed in Table II. In addition, the maximum weight loss rate of two PC/10PES/PSiA is lower than that of PC. It is regarded that the degradation pathway of PC and PES matrix is greatly varied by PSiA and the degraded process and products of PC/10PES/PSiA are quite different from those of PC and PC/10PES. Small amounts of PSiA induce a lower char yield at 650°C than that of PC/10PES, but the formed carbon layer of two PC/10PES/PSiA develops higher flame retardant effect.

TGA–FTIR analysis

TGA–FTIR analysis of PC, PES, PC/10PES, and PC/10PES/0.5PSiA are conducted to estimate the function of PES and PSiA. Their TGA curves in Figure 8 are slightly different from TGA curves in Figures 5 and 7 due to different instruments. Spectral variations of PC can be observed during heating from 420


×2000   ×10000
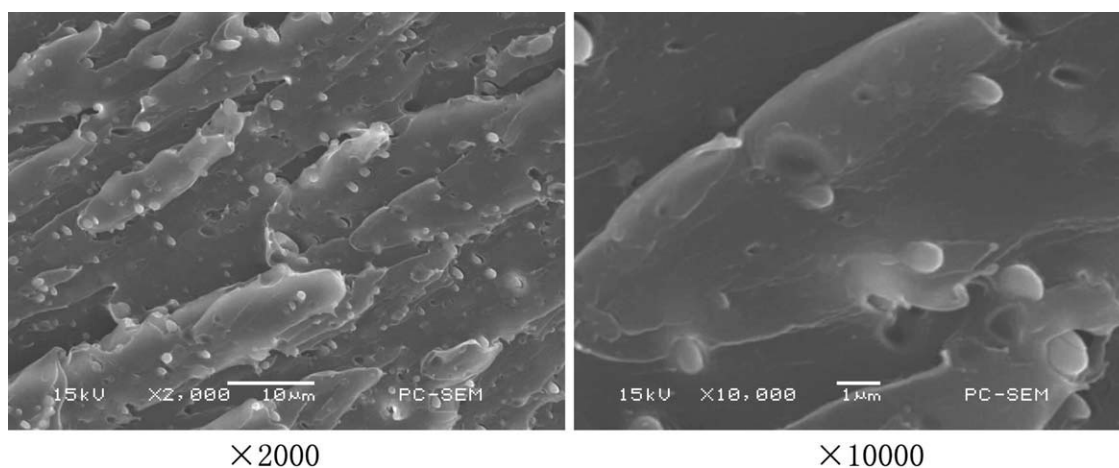
Figure 4 SEM micrographs of impact-fractured surface of PC/10PES/0.5PSiA.
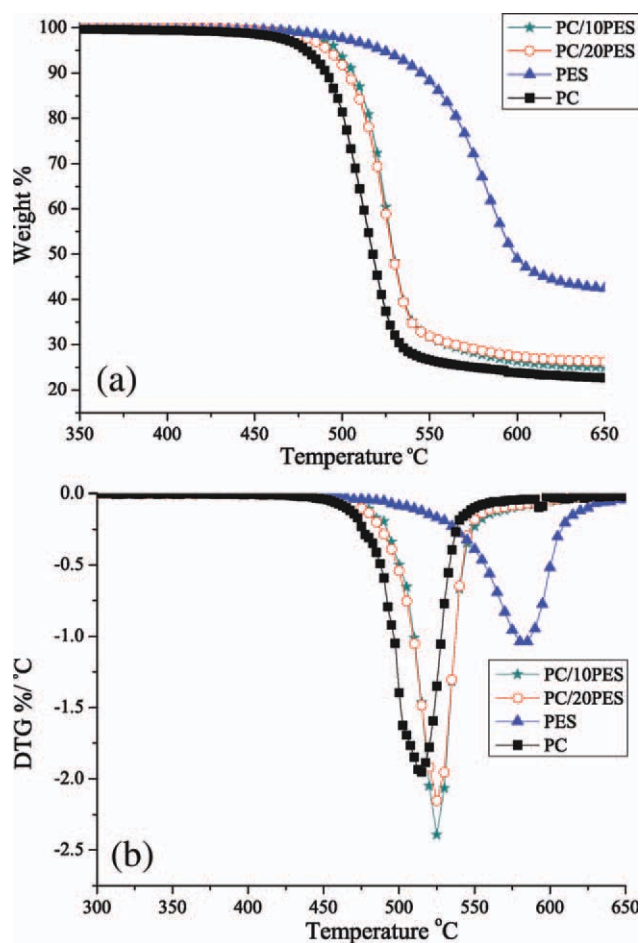
Figure 5 TGA and DTG curves of PC, PES and two PC/PES blends in N_2 at a heating rate of 20°C/min. [Color figure can be viewed in the online issue, which is available at wileyonlinelibrary.com.]

to 550°C and the generation of CO_2 and H_2O is found over the whole range. FTIR spectra of evolved volatile components of PC in the regions of 1650–1100 cm^{-1} with 10%, 20%, 40%, 60%, 70%, and 77%
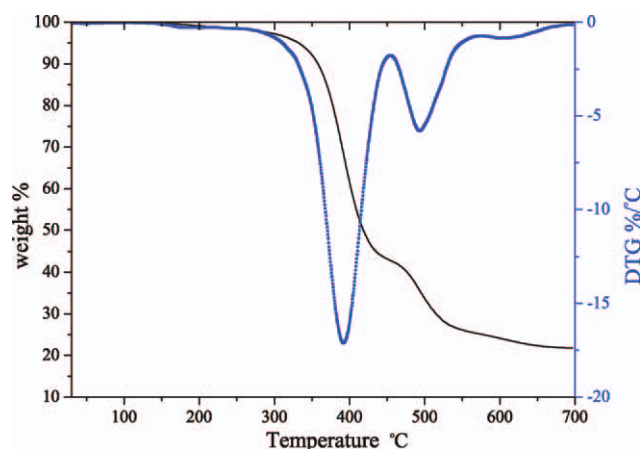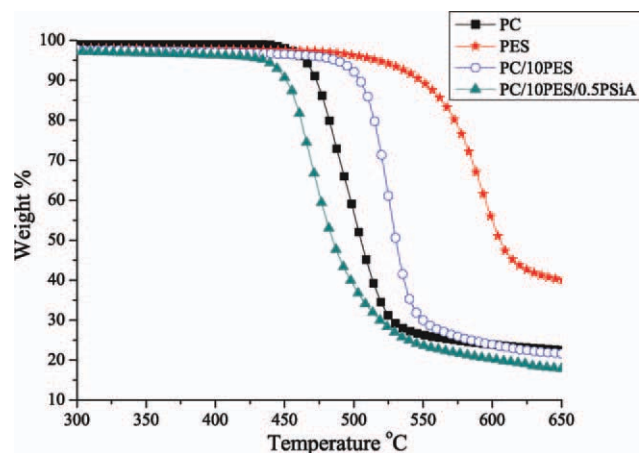

Figure 6 TGA and DTG curves of PSiA in N_2 at a heating rate of 20°C/min. [Color figure can be viewed in the online issue, which is available at wileyonlinelibrary.com.]
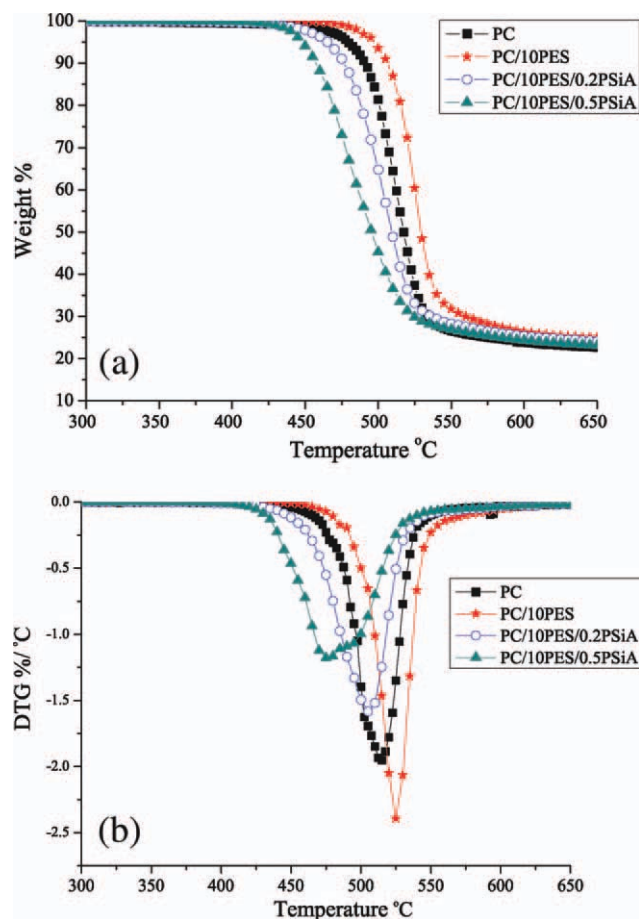
**Figure 7** TGA and DTG curves of PC, PC/10PES, and two PC/10PES/PSiA in N_2 at a heating rate of 20°C/min. [Color figure can be viewed in the online issue, which is available at wileyonlinelibrary.com.]

weight loss are shown in Figure 9. The peaks at 1604 and 1508 cm^{-1} correspond to the skeletal vibration and C—H stretching of phenyl group. The peak at 1260 cm^{-1} is attributed to aromatic ether stretching
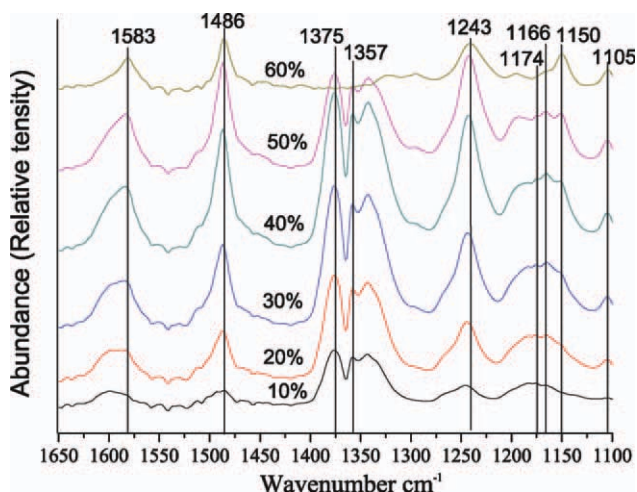

Figure 8 TGA curves of PC, PES, PC/10PES, and PC/10PES/PSiA in N_2 at a heating rate of 20°C/min. [Color figure can be viewed in the online issue, which is available at wileyonlinelibrary.com.]
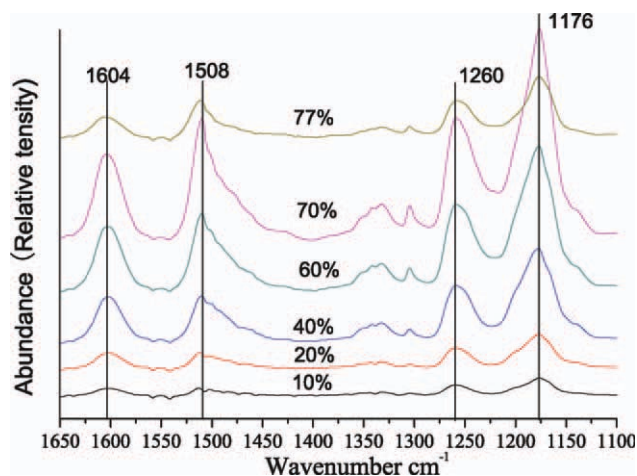
Figure 9 FTIR spectra of evolved volatiles from PC at different weight loss. [Color figure can be viewed in the online issue, which is available at wileyonlinelibrary.com.]

and the peak at 1176 cm^{-1} is ascribed to carbonhydroxy (Ar—O) stretching of aliphatic substituted phenols.[20] Most of absorption peaks become more intensive with the increase in weight loss until 70%.

Thermal degradation of PES occurs at higher temperature range (480–620°C) and main evolved products are SO$_2$, phenol, diphenyl sulfone, and diphenyl ether.[7,8] FTIR spectra of evolved volatile components with 10%, 20%, 30%, 40%, 50%, and 60% weight loss in the regions 1650–1100 cm^{-1} are shown in Figure 10. Major peaks are attributed to (1) phenyl group: 1583 and 1486 cm^{-1} (skeletal vibration and C—H deformation), (2) SO$_2$: 1375, 1357 cm^{-1} (S=O symmetrical stretching) and 1166, 1150 cm^{-1} (S=O asymmetrical stretching),[21] (3) aromatic ether: 1243 cm^{-1} (C—O stretching), and (4) phenols: 1174 cm^{-1} (C—OH stretching). The growth of almost all bands is observed until 40% of weight loss.

Comparing the spectra of evolved volatiles from PC and PES, the peaks at 1375 and 1357 cm^{-1} ascribed to SO$_2$ seem to be unique to PES. Several major characteristic peaks originating from aromatic ether, phenols, and phenyl group slightly shift to lower wavenumber in the spectra of PES. The peaks attributed to aromatic ether stretching and phenolic C—OH stretching shift from 1260 and 1176 cm^{-1} of PC to 1243 and 1166 cm^{-1} of PES, respectively. The skeletal vibration and C—H stretching of phenyl group shift from 1604 and 1508 cm^{-1} to 1583 and 1486 cm^{-1}. The above absorptions are used for distinguishing evolved volatiles of PES from those of PC.

FTIR spectra of evolved volatiles from PC/10PES and PC/10PES/0.5PSiA at various weight losses in the regions 1650–1110 cm^{-1} are shown in Figure 11. It can be found that most of the absorption positions and variation trend with the weight loss are similar with those of PC, suggesting a dominant
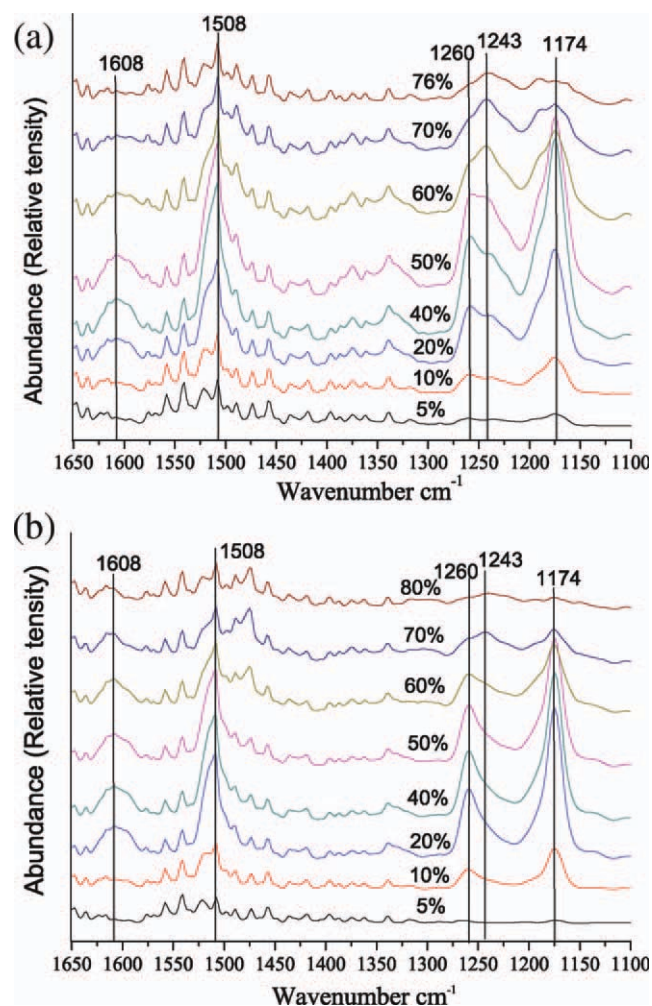
Figure 11 FTIR spectra of evolved volatiles from PES/10PES (a) and PC/10PES/0.5PSiA (b) at different weight loss. [Color figure can be viewed in the online issue, which is available at wileyonlinelibrary.com.]

Figure 10 FTIR spectra of evolved volatiles from PES at different weight loss. [Color figure can be viewed in the online issue, which is available at wileyonlinelibrary.com.]
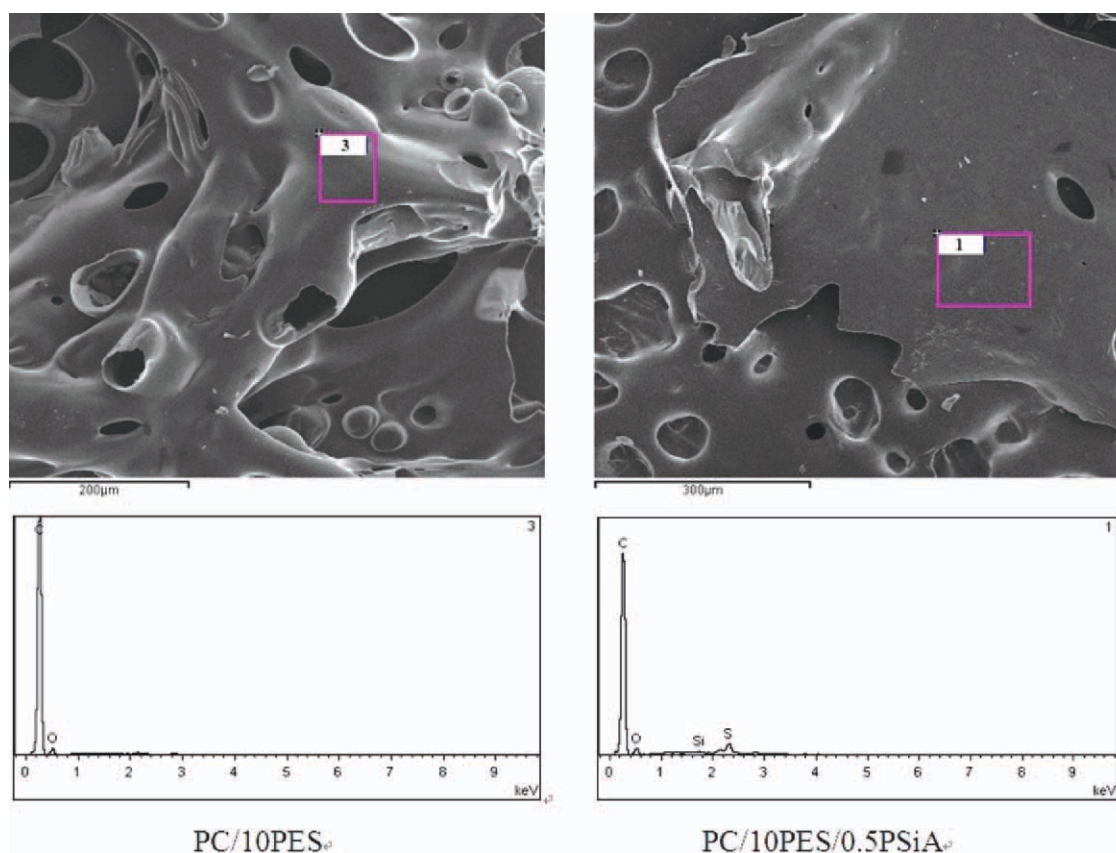
Figure 12 SEM/EDS micrographs of the residue surface of PC/10PES and PC/10PES/0.5PSiA from an extinguished specimen. [Color figure can be viewed in the online issue, which is available at wileyonlinelibrary.com.]

degradation from PC. It is difficult to discern the degradation mode of two blends from the occurrence of SO_2 owing to weak absorptions of S=O stretching at 1375 and 1357 cm^{-1}. But there are obvious differences in the absorption variation of 1260 and 1243 cm^{-1}. For PC/10PES, the 1243 cm^{-1} peak originating from PES is accompanied with the appearance of 1260 cm^{-1}, indicating that PC and PES simultaneously begin to lose weight. Due to the continuous degradation of PES it is given the speculation that the charring function of PES in the condensed phase is quite minimal. For PC/10PES/0.5PSiA, however, only a single 1260 cm^{-1} peak appears and the 1243 cm^{-1} peak is not evident until 60% weight loss at 519°C in the spectrum, implying that PSiA dominantly promotes the PC degradation and engenders little effect on PES. As a result, degraded products of PC have an opportunity to combine with PES to form a superior flame-retarded carbon layer with enriched sulfur. Higher sulfur content on the residue surface is detected by the followed SEM/EDS analysis. From TGA–FTIR analysis it can be concluded that the degradation mode of PC/10PES/0.5PSiA is more advantageous to superior flame retardance than that of PC/10PES.

SEM/EDS analysis of residue surface

SEM morphologies of residue surface from an extinguished specimen of PC/10PES and PC/10PES/0.5PSiA via vertical burning tests are displayed in Figure 12. It can be exposed that there are more hollows in the char structure of PC/10PES. Obviously, the carbon layer of PC/10PES/0.5PSiA can shield more firmly the underlying polymer from attacking of oxygen and radiant heat. In addition, a larger difference lies in the corresponding elemental distributions detected from SEM/EDS (Table V). Apart from C and O element, sulfur content of 2.25 wt % and silicon content of 0.32 wt % are determined on the residue surface of PC/10PES/0.5PSiA. On the authority of 10.0 wt % PES (sulfur content of PES is 10–11%) and 0.5 wt % PSiA loadings, sulfur content is about 1 wt % while silicon content can be neglected in two blends before burning. A higher

TABLE V
Elements Analysis of Residual Chars of PC/PES and PC/PES/PSiA

Elements	Weight (%)			
	C	O	S	Si
PC/10PES	90.95	9.05	0	
PC/10PES/0.5PSiA	88.93	8.51	2.25	0.32

sulfur content than the theoretical value strongly supports the speculation on the relative stability of PES under the action of PSiA drawn from TGA–FTIR analysis. Higher silicon content confirms its accumulation in the condensed phase. The carbon layer containing more sulfur element takes on higher resistance to the high temperature and silicon element is credited to further improving its thermal oxidative stability.[22,23] Therefore, PC/10PES/0.5PSiA exhibits better flame retardant effect.

CONCLUSIONS

The UL 94 rating of PC/10PES was elevated to V-0 for 1.6-mm thick samples by the addition of 0.5 wt % PSiA (PC/10PES/0.5PSiA) in the premise of retaining the high toughness and rigidity of PC. The flammability characteristics of PC/10PES/0.5PSiA in a cone calorimeter measurement was decreased. The distribution of PES in the PC matrix was significantly modified by the incorporation of 0.5 wt % PSiA from SEM morphologies of impact-fractured surfaces. PSiA dominantly promoted the PC degradation and the degraded products were combined with PES to form a superior flame-retarded carbon layer in PC/10PES/0.5PSiA according to TGA–FTIR analysis results. The accumulation of sulfur and silicon element on the residue surface after vertical burning tests of PC/10PES/0.5PSiA was detected by SEM/EDS. The forceful synergy of PES and small amounts of PSiA provided a promising alternative for halogen-free flame-retarded approach of PC.

References

1. Levchik, S. V.; Weil, E. D. Polym Int 2005, 54, 981.
2. Wold, C.; Van de Grampel, R. Polym Test 2009, 28, 495.
3. Nodera, A.; Kanai, T. J Appl Polym Sci 2004, 94, 2131.
4. Ballistreri, A.; Montaudo, G.; Scamporrino, E. J Polym Sci Part A: Polym Chem 1988, 26, 2113.
5. Xu, L.; Weiss, R. A. Polym Degrad Stab 2004, 84, 295.
6. Wang, Y. Z.; Yi, B.; Wu, B.; Yang, B.; Liu, Y. J Appl Polym Sci 2003, 89, 882.
7. Perng, L. H. J Appl Polym Sci 2001, 81, 2387.
8. Perng, L. H. J Polym Sci Part A: Polym Chem 2000, 38, 583.
9. Wang, Z. G.; An, L. J.; Wang, X. H. J Macromol Sci B 1998, 37, 717.
10. Jiang, D.; Zhang, S. L.; Yang, Y. H.; Jiang, Z. H.; Ma, R. T. J Macromol Sci B 2008, 47, 1.
11. Hamdani, S.; Longuet, C.; Perrin, D.; Lopez-Cuesta, J. M.; Ganachaud, F. Polym Degrad Stab 2009, 94, 465.
12. Zhao, J. Q.; Fu, Y.; Liu, S. M. Polym Polym Compos 2008, 16, 471.
13. Hsiue, G. H.; Liu, Y. L.; Tsiao, J. J Appl Polym Sci 2000, 78, 1.
14. Iji, M.; Serizawa, S. Polym Adv Technol 1998, 9, 593.
15. Dang, X. R.; Bai, X.; Zhang, Y. J Appl Polym Sci 2011, 119, 2730.
16. Perret, B.; Schartel, B. Polym Degrad Stab 2009, 94, 2204.
17. Fu, Y.; Liu, S. M.; Sun, H. Y.; Ye, H.; Zhao, J. Q. Petrochem Technol 2008, 37, 941.
18. Kolarik, J.; Fambri, L. Macromol Mater Eng 2000, 283, 41.
19. Liu, S. M.; Lang, X. M.; Ye, H.; Zhang, S. J.; Zhao, J. Q. Eur Polym J 2005, 41, 996.
20. Politou, A. S.; Morterra, C.; Low, M. J. D. Carbon 1990, 28, 529.
21. Pei, X. Q.; Wang, Q. H.; Chen, J. M. Appl Surf Sci 2006, 252, 3878.
22. Liu, Y. L.; Chang, G. P.; Wu, C. S., Chiu, Y. S. J Polym Sci Part A: Polym Chem 2005, 43, 5787.
23. Liu, Y. L.; Chou, C. I. Polym Degrad Stab 2005, 90, 515.